Available online at www.sciencedirect.com

SciVerse ScienceDirect

Journal of the European Ceramic Society 32 (2012) 671–680

www.elsevier.com/locate/jeurceramsoc

Phase equilibria and electrical properties of pyrochlore and zirconolite phases in the Bi_2O_3–ZnO–Ta_2O_5 system

C.C. Khaw [a,*], K.B. Tan [b], C.K. Lee [c], A.R. West [d]

[a] *Universiti Tunku Abdul Rahman, Department of Mechanical and Material Engineering, 53300 Setapak, Kuala Lumpur, Malaysia*
[b] *Universiti Putra Malaysia, Department of Chemistry, 43400 Serdang, Selangor, Malaysia*
[c] *Academic Science Malaysia, 902-4 Jalan Tun Ismail, 50480 Kuala Lumpur, Malaysia*
[d] *University of Sheffield, Department of Materials Science and Engineering, Mappin St, Sheffield S1 3JD, UK*

Received 21 April 2011; received in revised form 29 September 2011; accepted 1 October 2011
Available online 27 October 2011

Abstract

The complete subsolidus phase diagram of the system Bi_2O_3–ZnO–Ta_2O_5, including cubic pyrochlore and monoclinic zirconolite phases, has been determined at 950–1050 °C. Through systematic heat treatment and X-ray diffraction of over 100 compositions, the layout of compatibility triangles (both 2-phase and 3-phase) and single phase solid solution areas has been determined. Pyrochlore and zirconolite phases have ideal nominal compositions $Bi_{1.5}Zn_{1.0}Ta_{1.5}O_7$ and $Bi_2(Zn_{1/3}Ta_{2/3})_2O_7$ respectively, but both form solid solution areas. The sintering condition of pyrochlore pellets has been optimised to obtain high density ceramics with minimal weight loss: optimised condition is 1100 °C for pellets covered with sacrificial powder. Permittivity, ε' dielectric loss and temperature coefficient of capacitance, TCC, of single phase materials were measured using impedance spectroscopy; ε' and TCC show little variation with composition but the losses are higher for Zn-deficient compositions.

Keywords: Powder solid-state reaction; Sintering; X-ray methods; Electrical properties; Tantalates

1. Introduction

Pyrochlore phases have many potential application areas due to their wide spectrum of electrical, magnetic, optical and catalytic properties. These properties are normally controlled by ionic size, polarisability and electronic configuration parameters and sometimes by the preparation and fabrication conditions. Pyrochlores can be used as solid electrolytes, oxygen electrodes, and catalysts and in active or passive electronic applications such as high permittivity ceramics, thermistors, gas sensors, switching elements, thick film resistors and materials for screen printing.[1,2] They play a role in nuclear waste disposal and can be used as semiconductor electrodes for solar energy conversion.[3]

Pyrochlore and zirconolite-related phases in the Bi_2O_3–ZnO–Ta_2O_5/Nb_2O_5 (referred to as BZT and BZN) systems have attracted considerable interest recently due to their favourable combination of electrical properties, coupled with low firing temperatures, for capacitor and high-frequency filter applications. Historically, development of microwave dielectrics has focused on materials with high quality factor, Q (defined as the reciprocal of dielectric loss) with $Q > 10{,}000$. However, device manufacturers have more recently emphasised compatibility with low resistivity metals during processing and considered the use of lower Q dielectrics, $Q \approx 200$. This change in material needs has led to the development of several new classes of high frequency dielectric ceramics. Ceramics based on BZN and BZT ternary systems containing pyrochlore and zirconolite two-phase mixtures are promising dielectrics because of their suitable Q values and also their TCC can be compositionally controlled to achieve a low value.[4,5]

BZN pyrochlore has a high permittivity, ε', of ~150 and a low dielectric loss, with $\tan\delta$ ~0.0005 at 1 MHz, but a large negative TCC, ~−500 ppm/°C. BZT pyrochlore has ε' ~71 and $\tan\delta < 0.005$ at 1 MHz.[5–10] In both systems, the pyrochlore phase occupies a solid solution area on the phase diagram,[11–13] but little information is available on possible composition-dependence of the electrical properties. Ling et al.[14] studied the dielectric properties of a series of

* Corresponding author. Tel.: +60 341079802; fax: +60 341079803.
E-mail address: khawcc@utar.edu.my (C.C. Khaw).

0955-2219/$ – see front matter © 2011 Elsevier Ltd. All rights reserved.
doi:10.1016/j.jeurceramsoc.2011.10.012

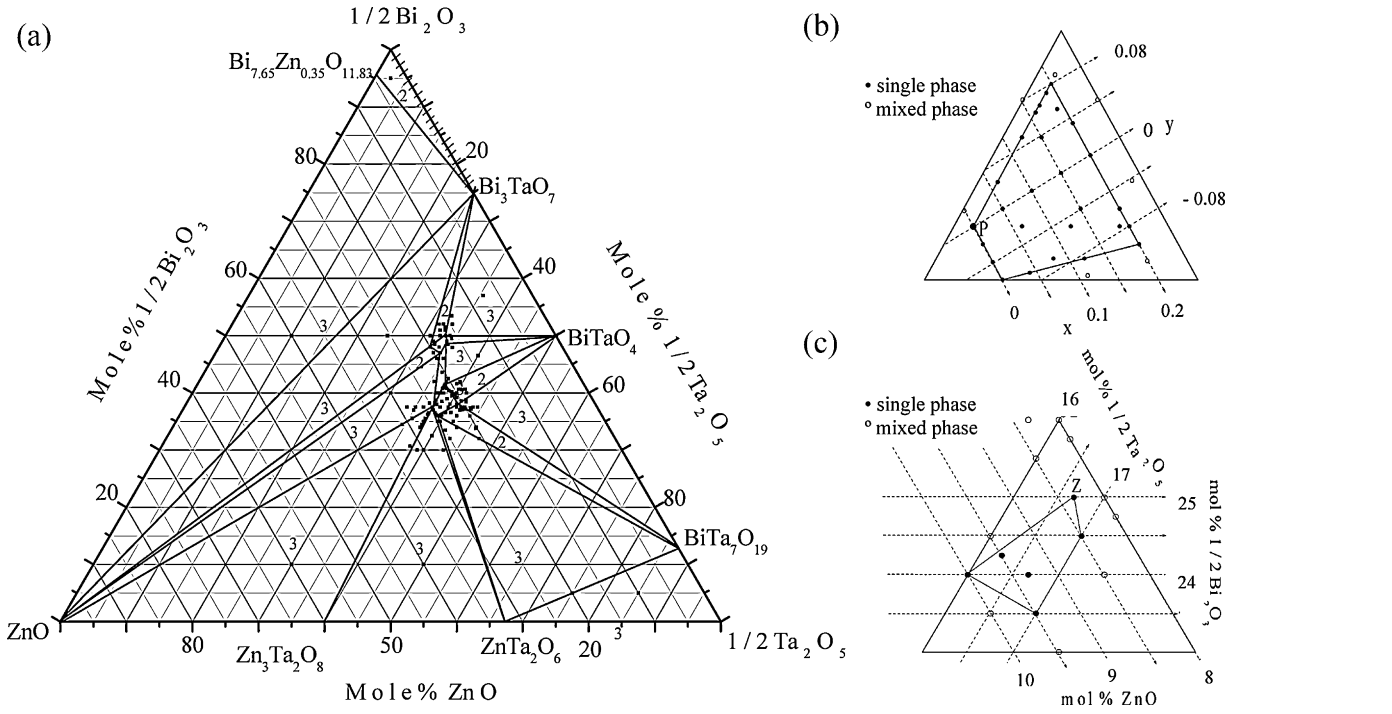

Fig. 1. (a) Overall phase diagram of the Bi_2O_3–ZnO–Ta_2O_5 ternary system; numbers in each compatibility triangle refer to the number of phases. (b) Expanded pyrochlore area with x and y as variables in the formula, $Bi_{1.5+y/2}Zn_{1.0-x/2}Ta_{1.5-y/2}O_{7-x/2-y/2}$. (c) Expanded zirconolite area with mol% of Bi_2O_3, ZnO and Ta_2O_5 shown.

compositions in the Bi_2O_3–NiO–ZnO–Nb_2O_5 system consisting of $xBi_3(Ni_2Nb)O_9 + (1-x)Bi_2(ZnNb_{2(1+\delta)})_yO_{3+6y+5\delta y}$ and found that compositional changes significantly alter the dielectric properties. Several approaches were used in their study: (1) with fixed $x = 0.265$, varying y ($0.8 \le y \le 1.1$) and δ ($-0.05 \le \delta \le 0.05$), ε' increased and TCC decreased with increase of y and δ while there was little variation of dielectric loss with $\tan\delta < 0.005$ for most compositions; (2) with fixed $x = 0.265$, $y = 0.8$ and varying δ ($-0.05 \le \delta \le 0.05$), ε' increased and TCC decreased with increase of δ whereas dielectric losses were almost constant; (3) with fixed $y = 0.8$, $\delta = 0$ and varying x ($0 \le x \le 1$), ε' and $\tan\delta$ decreased initially and then increased when $x = 0.5$ and 0.265, respectively, but no systematic variation of TCC with x was found. Wang et al.[15] showed that for $xBi_{1.5}Zn_{0.5}(Zn_{0.5}Nb_{1.5})O_7 + (1-x)Bi_{3/4}Nb_{1/4}O_{7/4}$ ($0.05 \le x \le 0.35$) ceramics biphasic mixtures of $Bi_2(Zn_{1/3}Nb_{2/3})_2O_7$ (β phase) and $Bi_{3/4}Nb_{1/4}O_{7/4}$, a distorted cubic fluorite (F), were obtained for $x = 0.05$–0.3. The permittivity and dielectric loss of β–F ceramics decreased with x whereas TCC values appeared to increase with x.[7,14] The zirconolite phases of nominal stoichiometry, $Bi_2Zn_{2/3}Nb_{4/3}O_7$ and $Bi_2(Zn_{1/3}Ta_{2/3})_2O_7$, appear to have variable composition that, as yet, has not been well characterised. BZT zirconolite has $\varepsilon' = \sim 61$, $\tan\delta < 0.001$ and TCC = +60 ppm/°C at 1 MHz.[6,12] BZN zirconolite has, $\varepsilon' = \sim 80$, $\tan\delta = 0.0001$ and TCC ~+200 ppm/°C.[7,15,16] Of particular interest for applications requiring temperature stability of electrical characteristics is to make composites of the pyrochlore and zirconolite phases and adjust their relative amounts so that the net TCC is close to zero.

The components of the Bi_2O_3–ZnO–Ta_2O_5/Nb_2O_5 systems are two unreactive oxides, Ta_2O_5/Nb_2O_5 and ZnO, together with one volatile, reactive oxide Bi_2O_3. In order to prepare samples and obtain phases or phase mixtures that represent thermodynamic equilibrium, it is necessary to find appropriate heat treatment conditions such that the temperature is high enough for Ta_2O_5/Nb_2O_5 and ZnO to react, but not too high that volatilisation of Bi_2O_3 occurs before it can be combined chemically.

The subsolidus phase diagram of the system Bi_2O_3–ZnO–Ta_2O_5 in the region of the cubic pyrochlore phase has been reported previously.[13] The pyrochlore forms a compositional or solid solution area in the phase diagram, rather similar in size and location to that in the Nb_2O_5 system,[11] but in this case including the ideal composition $Bi_{1.5}Zn_{1.0}Ta_{1.5}O_7$, marked as point 'P' in Fig. 1(b). A phase diagram containing pyrochlore and zirconolite, $Bi_2Zn_{2/3}Nb_{4/3}O_7$, phases in the BZN system was presented previously by ourselves[11,17,18] and Vanderah et al.,[12] and the two diagrams showed reasonably good agreement.

The only previous attempt to investigate the phase diagram for the BZT system was a detailed study of the join between the stoichiometric compositions of pyrochlore (α) and zirconolite (β).[8] This join was represented by the general formula $(Bi_{3x}Zn_{2-3x})(Zn_xTa_{2-x})O_7$ ($0.5 \le x \le 0.67$). The crystal structure gradually transformed from β to α with decreasing x. There was a (α + β) coexisting two phase region between the two single phase end-member regions. Clear evidence was obtained for a limited range of cubic pyrochlore solid solutions[8]; however, since there was also evidence that Bi_2O_3 volatilisation

occurred, the true locus of the solid solutions was unclear and indeed, may have departed from the line connecting pyrochlore and zirconolite compositions. Such a conclusion would be fully consistent with the results reported previously,[13] since the Bi-rich edge of the solid solution area does not coincide with the pyrochlore–zirconolite join. Hence, compositions on the pyrochlore–zirconolite join, which were initially biphasic, could become single-phase by loss of Bi_2O_3, which would take them to compositions coinciding with the edge of the pyrochlore solid solution area.

One objective of the present paper has been to determine the complete subsolidus phase diagram of the BZT system. A second objective was to optimise processing conditions to avoid loss of Bi_2O_3 by volatilisation, prepare single phase products and obtain ceramics of low porosity for property measurements.

2. Materials and methods

Bi Zn tantalate materials were prepared by solid-state reaction of mixtures of Bi_2O_3 (99.9%, Aldrich), ZnO (99%, Merck), and Ta_2O_5 (99.993%, Alfa-Aesar); Bi_2O_3 was dried at 300 °C for 1–2 h, while ZnO and Ta_2O_5 were dried at 600 °C for 2–3 h before weighing. Compositions (3–4 g total) were mixed with acetone in an agate mortar, dried, and fired in Pt foil boats at 750–1050 °C for 2 days, with intermediate regrinding. Weight-loss checks showed no significant loss and therefore, no volatilisation of the starting materials. The samples were analysed by X-ray powder diffraction (XRD) with a Shimadzu diffractometer XRD 6000, CuKα radiation in the 2θ range 10–70° at 2°/min. Data for cell parameter determination were collected at a scan rate of 0.1°/min.

To determine the equilibrium phase diagram of the BZT system, samples of more than 100 different compositions were heated in a step-wise cycle, with lower temperature stages used to ensure initial reaction of the Bi_2O_3. Ta_2O_5 is less reactive than Nb_2O_5 and it was found that BZT samples generally required heating at 50–100 °C higher than corresponding BZN samples in order to achieve a comparable level of reaction. Thus, from the results of heating for various times and at temperatures in the range 800–1100 °C, it was found that a phase-pure cubic pyrochlore phase was formed after heating BZT compositions for 48 h at 1050 °C whereas 950 °C was sufficient for BZN. Zirconolite, with higher bismuth content than pyrochlore was fully formed at lower temperatures, ∼950 °C in the BZT system; this shows that appropriate reaction temperatures were also composition-dependent.

A complete subsolidus phase diagram of the system Bi_2O_3–ZnO–Ta_2O_5 was constructed, by ensuring that the samples had reached equilibrium: samples were heated until there were no further changes in the phase/phase assemblages, either at the same temperature, or on subsequently raising the temperature by 25–50 °C. The synthesis temperature required to reach equilibrium was found, by trial and error, to gradually decrease from ∼1050 °C in low Bi regions towards ∼750 °C in Bi-rich regions.

Electrical properties were determined by impedance spectroscopy using a Hewlett-Packard Impedance Analyser HP 4192A in the frequency range 5 Hz to 13 MHz. Pellets were cold-pressed and sintered overnight at 1025–1100 °C; in some cases, they were covered with sacrificial powder of the same composition. Weight-loss checks showed a slight loss on firing at ≥1100 °C. Gold paste/platinum paste electrodes were fired on at 200–800 °C; In–Ga liquid alloy electrodes were applied at room temperature. Impedance measurements were made from room temperature (∼30 °C) to 850 °C in incremental steps of 50 °C on a heating cycle with 30 min equilibration time before each measurement. The samples were then left overnight at ∼800 °C and a cooling cycle performed the next day. Impedance data were normalised by the geometric factor of the samples and were corrected for the blank capacitance of the jig.

3. Results and discussion

3.1. The Bi_2O_3–ZnO–Ta_2O_5 subsolidus phase diagram

The occurrence of phases along the three binary edges are reported in ICDD data and the literature: Bi_2O_3–Ta_2O_5,[19] Bi_2O_3–ZnO[20,21] and ZnO–Ta_2O_5. However, little or no information is available on the stability of the phases and the phase diagrams of these binary systems. Through careful heat treatment and X-ray analysis of >100 compositions, the layout of compatibility triangles (both 2-phase and 3-phase) and single phase solid solution areas in the ternary BZT system was determined. A selection of results is summarised in Table 1 . These were used to construct the phase diagram shown in Fig. 1.

In our previous study on the BZT system,[13] only a partial subsolidus phase diagram in the region of the pyrochlore solid solution area was reported. This area is essentially trapezoidal in shape, for which two of the four edges are parallel and correspond to ZnO contents of $25 \pm 0.5\%$ and $21 \pm 0.5\%$, Fig. 1(b). This area is similar in size and location to that of the Nb_2O_5 system, but in this case, it includes the ideal nominal composition P, $Bi_{1.5}Zn_{1.0}Ta_{1.5}O_7$. The constancy of the ZnO content for these two limiting edges is a strong indicator that one of the component mechanisms that should be used in describing the solid solution area is substitution of Bi for Ta at a constant Zn content. This mechanism, of course, requires additional changes to preserve charge balance and it is presumed that the oxygen content adjusts so as to maintain electroneutrality. There are two compositional variables, therefore, the Bi/Ta ratio and ZnO content, in which Zn^{2+} and O^{2-} vacancies are created in Zn-deficient compositions. The solid solution, confirmed by density measurements, can be described using the general formula $Bi_{1.5+y/2}Zn_{1.0-x/2}Ta_{1.5-y/2}O_{7-x/2-y/2}$.

A complete subsolidus phase diagram including solid solution areas of the zirconolite and pyrochlore phases is shown in Fig. 1(a). One corner, Z, of the zirconolite area, Fig. 1(c), represents the nominal stoichiometric formula $Bi_2(Zn_{1/3}Ta_{2/3})_2O_7$. Indexed X-ray powder diffraction data for $Bi_2(Zn_{1/3}Ta_{2/3})_2O_7$ are given in Table 2.

We speculate that the zirconolite solid solution area can also be described in terms of the same two mechanisms used to describe the pyrochlore solid solutions i.e.: (i) variation of ZnO content and (ii) variation in Bi/Ta ratio. However, the shape of

Table 1
Results of phases present in compositions prepared in the Bi_2O_3–ZnO–Ta_2O_5 ternary system.

Symbol	Cation ratio			Phases present at 1050 °C, 48 h
	Bi	Zn	Ta	
68	45.00	21.00	34.00	P + ZnO + Z
67	42.00	22.40	35.60	P + ZnO + Z
94	40.00	30.00	30.00	P + ZnO + Z
97	46.50	13.50	40.00	P + $BiTaO_4$ + Z
39	42.50	20.00	37.50	P + $BiTaO_4$ + Z
50	41.90	20.60	37.50	P + $BiTaO_4$ + Z
18	35.00	25.00	40.00	P + $ZnTa_2O_6$ + $BiTa_7O_{19}$
9	33.00	25.00	42.00	P + $ZnTa_2O_6$ + $BiTa_7O_{19}$
13	32.00	25.00	43.00	P + $ZnTa_2O_6$ + $BiTa_7O_{19}$
26	32.50	27.50	40.00	P + $ZnTa_2O_6$ + $Zn_3Ta_2O_8$
19	30.00	27.00	43.00	P + $ZnTa_2O_6$ + $Zn_3Ta_2O_8$
91	10.00	40.00	50.00	P + $ZnTa_2O_6$ + $Zn_3Ta_2O_8$
27	36.50	26.00	37.50	P + ZnO + $Zn_3Ta_2O_8$
30	34.00	28.50	37.50	P + ZnO + $Zn_3Ta_2O_8$
92	10.00	60.00	30.00	P + ZnO + $Zn_3Ta_2O_8$
44	37.50	20.00	42.50	P + $BiTaO_4$ + $BiTa_7O_{19}$
47	37.50	18.75	43.75	P + $BiTaO_4$ + $BiTa_7O_{19}$
61	37.20	20.00	42.80	P + $BiTaO_4$ + $BiTa_7O_{19}$
75	36.00	20.00	44.00	P + $BiTa_7O_{19}$
69	34.00	20.00	46.00	P + $BiTa_7O_{19}$
70	32.00	20.60	47.40	P + $BiTa_7O_{19}$
98	42.00	18.50	39.50	P + $BiTaO_4$
41	40.00	20.00	40.00	P + $BiTaO_4$
84	37.50	20.60	41.90	P + $BiTaO_4$
17	35.50	29.00	35.50	P + ZnO
20	34.50	31.00	34.50	P + ZnO
65	40.00	23.00	37.00	P + Z
66	43.60	20.40	36.00	P + Z
57	35.00	25.40	39.60	P + $ZnTa_2O_6$
123	5.00	10.00	85.00	$BiTa_7O_{19}$ + $ZnTa_2O_6$ + Ta_2O_5
89	5.00	20.00	75.00	$BiTa_7O_{19}$ + $ZnTa_2O_6$

Symbol	Cation ratio			Phases present at 950 °C, 48 h
	Bi	Zn	Ta	
The following compositions were synthesised at 950 °C, 48 h				
105	53.50	14.00	32.50	Bi_3TaO_7 + $BiTaO_4$ + Z
101	52.00	14.67	33.33	Bi_3TaO_7 + $BiTaO_4$ + Z
121	50.00	19.00	31.00	Bi_3TaO_7 + ZnO + Z
90	50.00	40.00	10.00	Bi_3TaO_7 + $Bi_{7.65}Zn_{0.35}O_{11.83}$ + ZnO
109	52.00	16.00	32.00	Bi_3TaO_7 + Z
108	49.00	19.00	32.00	Bi_3TaO_7 + Z
113	50.00	16.00	34.00	$BiTaO_4$ + Z
122	49.50	16.00	34.50	$BiTaO_4$ + Z
117	47.00	20.00	33.00	ZnO + Z

Symbol	Cation ratio			Phases present at 750 °C, 48 h
	Bi	Zn	Ta	
Composition synthesised at 750 °C, 48 h				
124	95.00	2.50	2.50	Bi_3TaO_7 + $Bi_{7.65}Zn_{0.35}O_{11.83}$

Symbol	Cation ratio			x	y	Phases present at 1050 °C, 48 h
	Bi	Zn	Ta			
Single phase compositions of pyrochlore (1050 °C, 48 h)						
P	37.50	25.00	37.50	0.000	0.000	P
4	36.00	25.00	39.00	0.000	−0.120	P
31	37.50	23.75	38.75	0.131	−0.049	P
32	38.75	23.75	37.50	0.131	0.049	P
33	38.50	23.00	38.50	0.200	0.000	P

Table 1 (*Continued*)

Symbol	Cation ratio			*x*	*y*	Phases present at 1050 °C, 48 h
	Bi	Zn	Ta			
37	39.00	22.00	39.00	0.300	0.000	P
52	40.00	22.00	38.00	0.308	0.077	P
53	38.00	22.00	40.00	0.308	−0.077	P
38	41.25	21.25	37.50	0.381	0.144	P
43	37.50	21.25	41.25	0.381	−0.144	P
40	39.50	21.00	39.50	0.400	0.000	P
85	37.00	21.00	42.00	0.400	−0.200	P
86	41.50	21.00	37.50	0.400	0.160	P

Symbol	Cation ratio			Phases present at 950 °C, 48 h
	Bi	Zn	Ta	
Single phase compositions of zirconolite (950 °C, 48 h)				
Z	50.00	16.67	33.33	Z
102	48.00	18.67	33.33	Z
107	49.00	17.00	34.00	Z
110	48.50	19.00	32.50	Z
112	47.00	19.00	34.00	Z
118	48.00	20.00	32.00	Z

the area is not as well-defined as for the BZT pyrochlore or for the analogous BZN zirconolite.[17,18]

3.2. Electrical property measurements

BZT pyrochlore materials are dielectrics that have very low conductivity. Preliminary electrical property measurements showed that it was not possible to measure their conductivity below 600 °C.[22] Nevertheless, it has been possible to measure their permittivity at high frequencies at room temperature and above.

It was of interest to determine whether the bulk permittivity of the pyrochlore solid solution varies with composition and whether the permittivity increases or decreases with temperature. However, the permittivity was found to depend on sample processing or sintering conditions and hence it was necessary first to optimise the sintering conditions before systematic studies of composition dependence could be carried out. Investigations on possible variables that may contribute to permittivity data were therefore carried out.

Pellets of two single phase pyrochlore compositions $Bi_{1.5}Zn_{1.0}Ta_{1.5}O_7$ and $Bi_{1.5}Zn_{0.9}Ta_{1.5}O_{6.9}$ were sintered at temperatures in the range 1025–1125 °C, both uncovered and covered with powder of the same composition. The results, Figs. 2 and 3, show a good correlation between permittivity and pellet density but less correlation between permittivity and weight loss. Increase in permittivity values of both covered and uncovered pellets occurred in parallel with increase of pellet density; an increase in permittivity was observed irrespective of the magnitude of the weight loss from covered and uncovered pellets. Covered pellets generally yielded higher permittivity values with much reduced weight loss compared to uncovered pellets.

This seems to indicate that the mechanism of sintering and densification, which probably involves grain growth and reduction in overall surface area, is facilitated by heating in a closed environment; in particular, the higher vapour pressure of bismuth in covered pellets may lead to enhanced densification through a mechanism of either vapour phase-assisted or liquid phase-assisted matter transport.

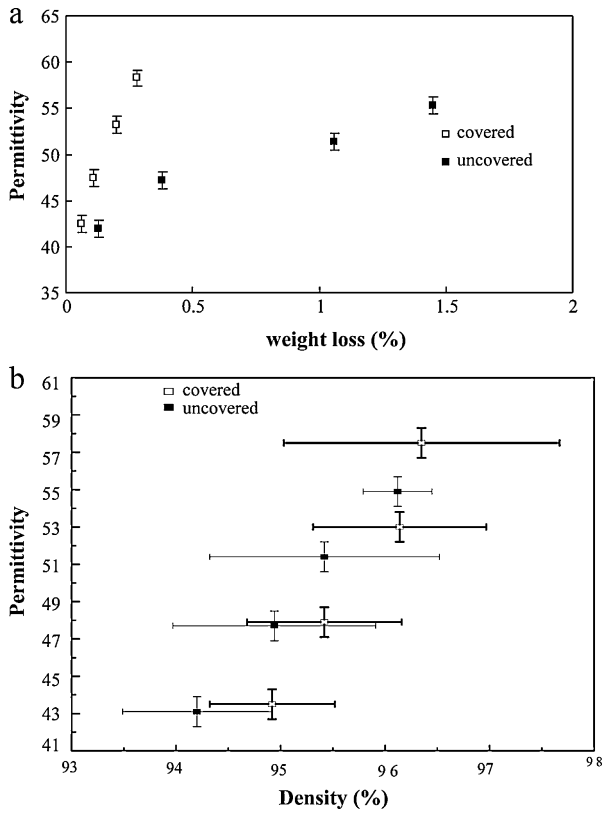

Fig. 2. Permittivity values of $Bi_{1.5}Zn_{1.0}Ta_{1.5}O_7$ (covered and uncovered) against (a) weight loss (%) and (b) density (%) at 30 °C, 1 MHz.

Table 2
Indexed X-ray diffraction pattern for $Bi_2(Zn_{1/3}Ta_{2/3})_2O_7$ zirconolite.

Refined lattice parameters
a: 13.105(3) Å
b: 7.6343(13) Å
c: 12.1816(19) Å
β: 101.210(17)
Volume: 1195.5(3) Å^3

h k l	I/I$_0$	*d* (obs) (Å)	*d* (calc) (Å)	*Δ* (2*θ*)
0 0 2	6.1	5.9772	5.9746	−0.0065
1 1 1	3.3	5.5260	5.5263	0.0010
−2 0 2	2.6	4.8796	4.8740	−0.0210
−1 1 2	2.8	4.6545	4.6544	−0.0005
2 0 2	3.1	4.0033	4.0050	0.0093
−3 1 1	2.0	3.7506	3.7522	0.0101
0 2 1	3.1	3.6350	3.6361	0.0077
−1 3 1	4.3	3.5648	3.5658	0.0068
3 1 1	2.5	3.4067	3.4057	−0.0080
−2 2 1	4.0	3.2478	3.2482	0.0034
2 2 1	100.0	3.0883	3.0875	−0.0079
0 0 4	31.6	2.9868	2.9873	0.0055
−2 2 3	32.4	2.6655	2.6661	0.0086
4 0 2	15.9	2.6263	2.6254	−0.0118
−4 2 1	1.6	2.4817	2.4820	0.0039
−4 0 4	1.7	2.4373	2.4370	−0.0049
2 2 3	3.4	2.4185	2.4179	−0.0102
−3 1 5	1.9	2.1885	2.1887	0.0039
5 1 2	1.6	2.1228	2.1235	0.0148
0 2 5	1.5	2.0271	2.0256	−0.0355
4 2 3	1.7	1.9646	1.9655	0.0212
0 4 0	8.7	1.9077	1.9086	0.0225
−3 1 6	19.1	1.8962	1.8960	−0.0060
−4 0 6	7.8	1.8630	1.8627	−0.0073
2 2 5	13.4	1.8463	1.8467	0.0105
−7 1 1	1.7	1.8162	1.8168	0.0190
−5 3 2	1.5	1.8016	1.8007	−0.0286
−1 1 7	1.5	1.6928	1.6935	0.0246
−4 4 2	7.7	1.6238	1.6241	0.0132
0 4 4	13.4	1.6088	1.6083	−0.0173
6 2 3	6.5	1.5911	1.5910	−0.0056
−2 2 7	5.8	1.5799	1.5800	0.0053
4 0 6	3.0	1.5624	1.5623	−0.0054
4 4 2	6.6	1.5440	1.5438	−0.0123
0 0 8	2.5	1.4937	1.4936	−0.0009
1 1 8	1.4	1.4261	1.4261	0.0023

These results show that the parameter that appears to be most important in controlling permittivity is the sample density. At the sintering temperature of 1125 °C, the density for $Bi_{1.5}Zn_{1.0}Ta_{1.5}O_7$, 96.41%, was almost the same as at 1100 °C, 96.35%, but with higher weight loss, 0.34%, compared to that at 1100 °C, 0.28%. Similar behaviour was seen for $Bi_{1.5}Zn_{0.9}Ta_{1.5}O_{6.9}$. Hence, the optimised sintering condition was set at 1100 °C and for pellets covered with powder.

The dielectric properties of $Bi_{1.5}Zn_{1.0}Ta_{1.5}O_7$ and pyrochlore solid solutions were investigated at various frequencies. Fig. 4 shows that between 100 kHz and 1000 kHz, little or no frequency dependence is observed in the range of 100–300 °C. The permittivity values are therefore regarded as intrinsic bulk values. Similar behaviour was observed in $Bi_{1.5}Zn_{1.0}Sb_{1.5}O_7$ ceramic.[23]

Using gold electrodes, no significant variation was seen with electrode-sample contact area and different measuring instruments. However, comparing data with gold, platinum and indium-gallium electrodes, gold was found to give higher permittivity values possibly due to its better wettability [Fig. 5(a) and (b)]. All the subsequent data reported in this study used gold electrodes.

Fig. 6(a) and (b) shows the variation of permittivity and dielectric loss for various compositions in the pyrochlore solid solution area using pellets sintered at 1100 °C. No clear trend in variation of permittivity with composition is observed. The permittivity of $Bi_{1.5}Zn_{1.0}Ta_{1.5}O_7$ is 58 at room temperature (30 °C) and 1 MHz, smaller than the reported value (∼71).[5,6,8] In the pyrochlore solid solutions most values were in the range 56–59, but scattered values as high as 69 and as low as 43

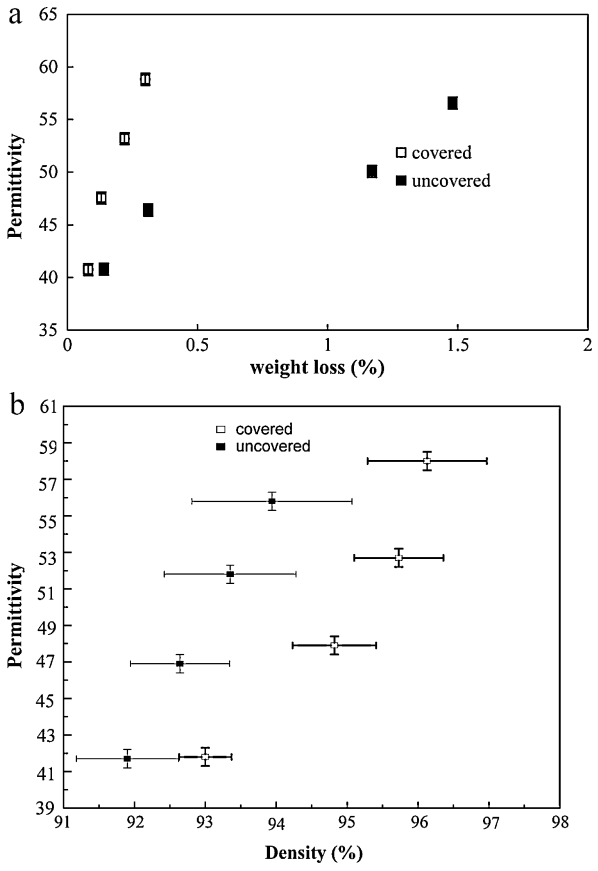

Fig. 3. Permittivity values of $Bi_{1.5}Zn_{0.9}Ta_{1.5}O_{6.9}$ (covered and uncovered) against (a) weight loss (%) and (b) density (%) at 30 °C, 1 MHz.

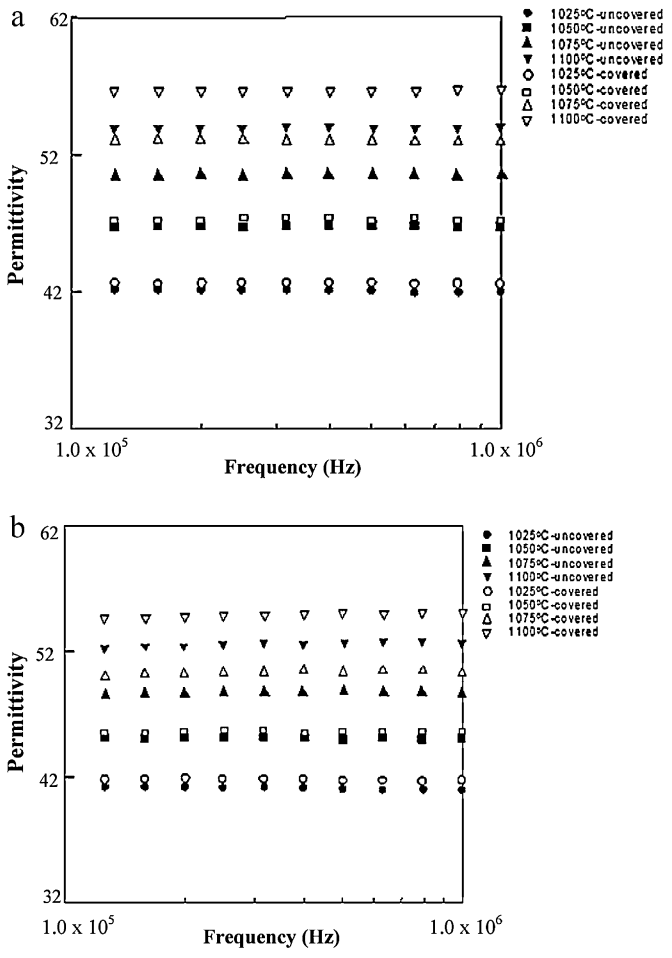

Fig. 4. Permittivity of $Bi_{1.5}Zn_{1.0}Ta_{1.5}O_7$ (covered and uncovered) at different sintering temperatures measured at (a) 30 °C and (b) 300 °C in the frequency range 100 kHz to 1 MHz.

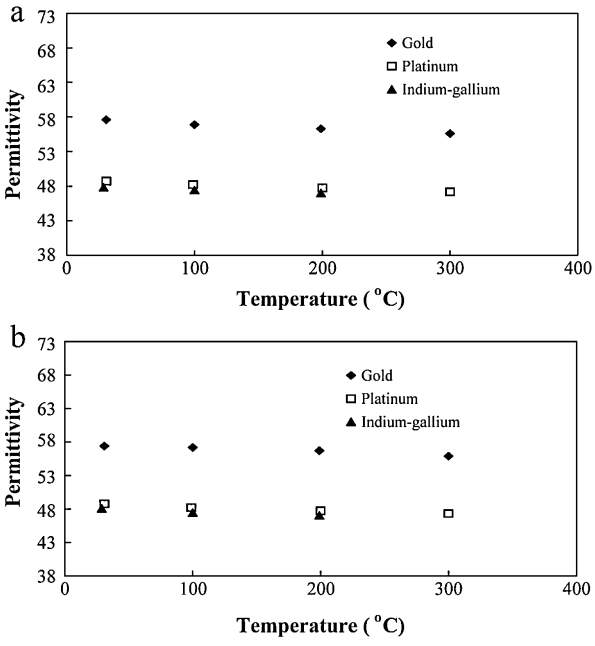

Fig. 5. Permittivity of $Bi_{1.5}Zn_{1.0}Ta_{1.5}O_7$ at (a) 1 MHz and (b) 100 kHz using 3 different electrodes.

were obtained; therefore, there is reasonable agreement with the literature value. The permittivity values are, in general, higher than those reported for bismuth zinc antimonate (BZS) (~32) but lower than those of BZN (~150).[7–9,24] The decrease in permittivity (Nb > Ta > Sb) could possibly be explained by a decrease in the total polarisability or a decrease in the molar volume.[25] For the present materials, and when Ta is substituted by Sb, there is a decrease in unit cell volume in the sequence BZN > BZT > BZS. It has been reported that dielectrics with high permittivity are based on structures with BO_6 octahedra joined at their apices.[25] The B ion, located in the centre of the octahedra, plays an important role in determining dielectric properties and in particular, a possible correlation between highly polarisable octahedra, high permittivity and high TCC values. Thus, in pyrochlore dielectrics, it is believed that there is a strong polarisation in NbO_6 octahedra resulting in high permittivity but relatively weak polarisation in SbO_6 octahedra leading to lower permittivity.[25,26]

Although no clear trend for variation of dielectric loss with composition is observed in BZT pyrochlore samples, all four compositions with stoichiometric Zn content, $x = 0$, have lower losses than Zn-deficient compositions, suggesting that Zn vacancies may act as a source of dielectric loss. Tan δ values are in the range $(1.5–8.5) \times 10^{-3}$, comparable to the reported value, $<5 \times 10^{-3}$.[5,6,12] Tan δ of α-BZT, $Bi_{1.5}Zn_{1.0}Ta_{1.5}O_7$, is 2.3×10^{-3} at 30 °C and 1 MHz. These tan δ values are

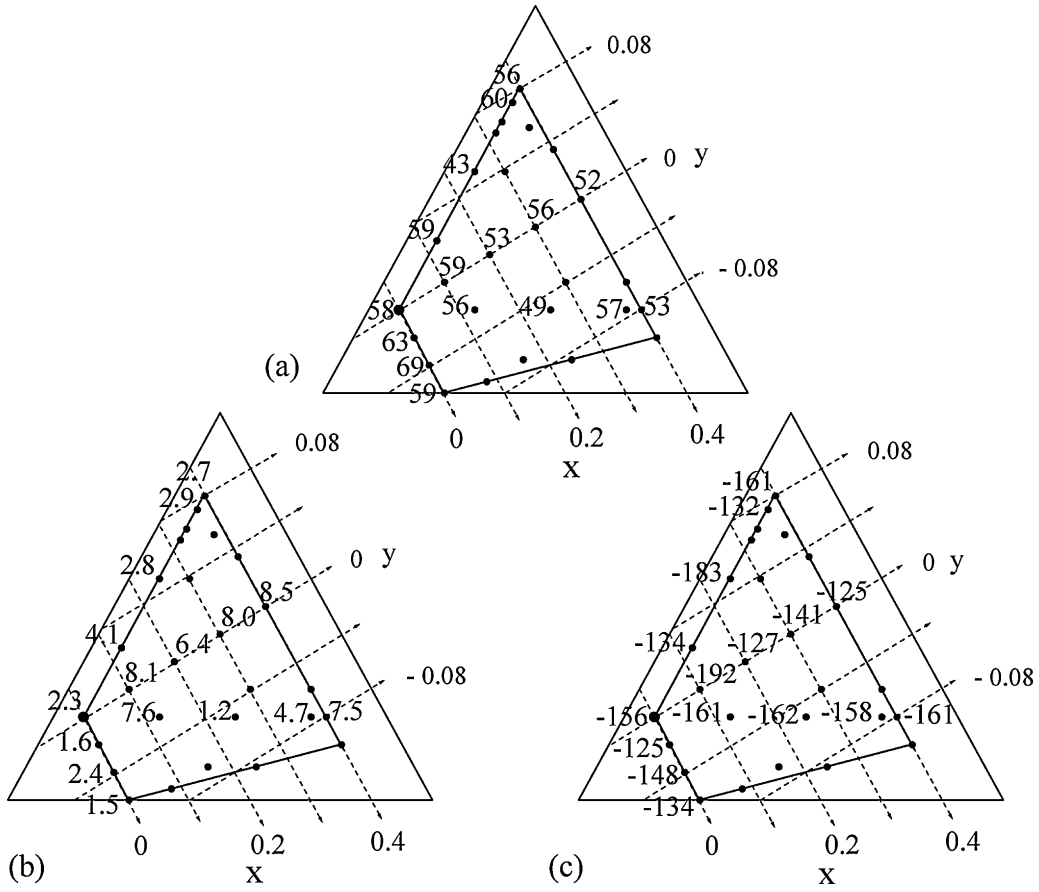

Fig. 6. Variation of (a) permittivity and (b) dielectric loss ($\times 10^{-3}$) and (c) TCC of compositions in the pyrochlore solid solution area at room temperature and 1 MHz.

comparable to those of BZS: 1×10^{-3}, but higher than those of BZN: 10^{-4}.[7,10,24]

The temperature coefficient of capacitance (permittivity), TCC, was calculated using the formula:

$$\mathrm{TCC} = C_{T_2} - \frac{C_{T_1}}{C_{T_1}(T_2 - T_1)} \quad (1)$$

where C_{T_1} is the measured capacitance at T_1 (room temperature, ~30 °C), and C_{T_2} is the measured capacitance at T_2, 300 °C.[7,27] Hence, an average value of TCC was calculated for the temperature range 30–300 °C. TCC obtained in this study for BZT pyrochlore is −156 ppm/°C measured at 1 MHz, comparable to −172 ppm/°C measured at 1 MHz. It is less negative than that of BZN pyrochlore ~−500 ppm/°C[7,9,10]; but more negative than that of BZS pyrochlore ~−100 ppm/°C.[25] Using the Electronic Industries Alliance (EIA) guidelines for temperature coefficients of NPO (negative positive zero) ceramic capacitor, capacitance change is observed over a standard temperature range of −55 to 125 °C.[10] Thus, in most researches of Bi-based pyrochlore materials with interest for applications requiring temperature stability of electrical characteristics, the change of capacitance is measured at a fixed frequency (1 MHz) with a LCR meter over the EIA temperature range, T_1 (room temperature, ~25 °C) to T_2 (125 °C) to calculate TCC. In our study, a broader temperature range was used, as there were insufficient data points in the EIA temperature range, Fig. 5. All the BZT, BZN and BZS pyrochlores have negative values of TCC. The TCC values as a function of BZT pyrochlore composition are shown in Fig. 6(c); there is no obvious correlation of TCC with composition.

The variation of permittivity, dielectric loss and TCC for various compositions in the zirconolite solid solution area using pellets sintered at 950 °C are shown in Fig. 7(a) and (b). No clear trend in variation of permittivity is observed. ε' of $Bi_2(Zn_{1/3}Ta_{2/3})_2O_7$ is 60 at 30 °C and 1 MHz, comparable to the reported value, ~61.[6,8] ε' values are, in general, lower than those of BZN ceramics, ~80,[7,15,16] consistent with lower polarisability of Ta than of Nb. To date, no zirconolite phase has been found in the BZS system.

No clear trend for variation of dielectric loss with composition is observed in BZT zirconolite samples, Fig. 7(b). All the solid solutions have tan δ in the order of 10^{-2}, except one at the edge of the area which has tan $\delta = 3 \times 10^{-3}$; tan δ of zirconolite BZT, $Bi_2(Zn_{1/3}Ta_{2/3})_2O_7$, is $<2.3 \times 10^{-2}$ at 30 °C and 1 MHz. These tan δ values are higher than those reported for BZT, 10^{-3} and BZN, 10^{-4}.[7,15,16]

TCC for BZT zirconolite is +75 ppm/°C measured at 1 MHz, Fig. 6(c), comparable to the reported value, +60 ppm/°C measured at 1 MHz.[6,8] It is smaller than that of monoclinic zirconolite BZN: ~+200 ppm/°C.[7,15,16] There is no obvious correlation of TCC with composition, Fig. 7(c).

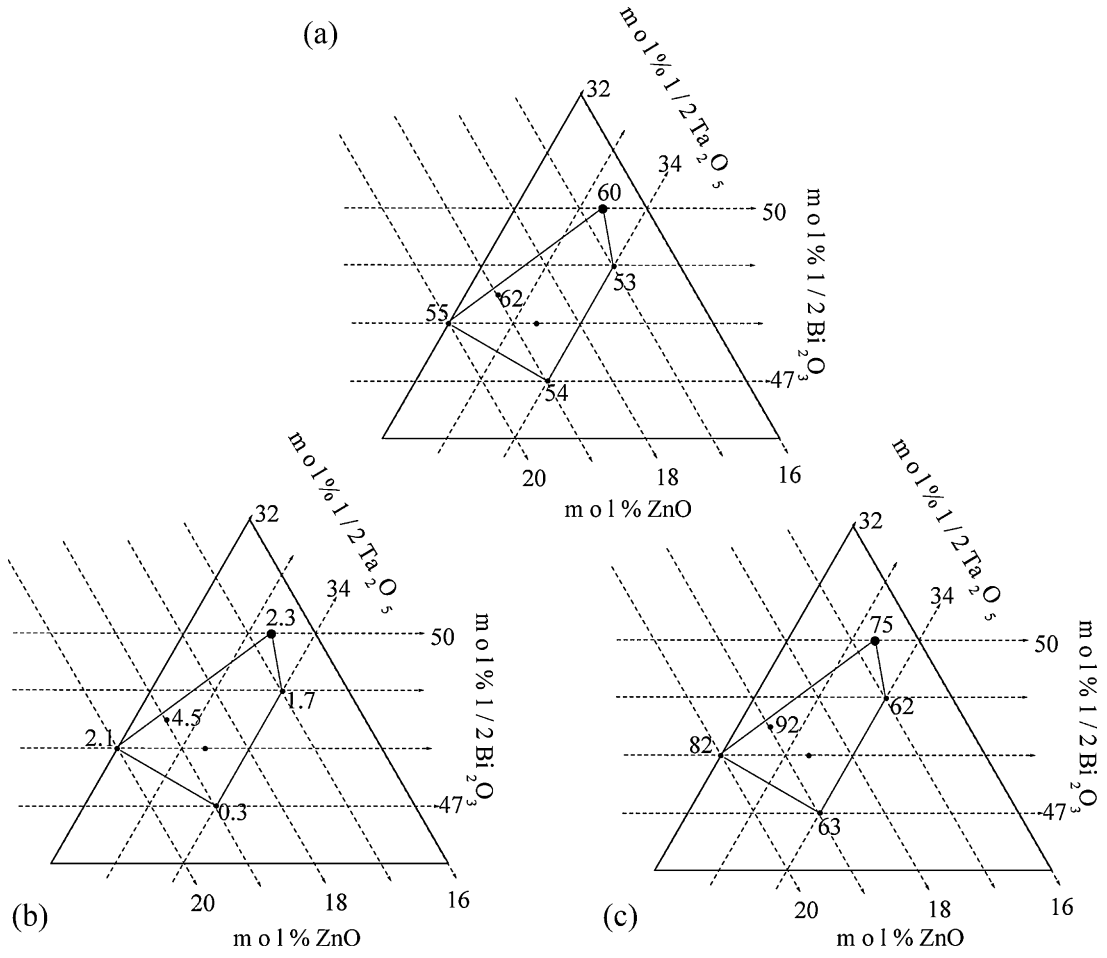

Fig. 7. Variation of (a) permittivity, (b) dielectric losses ($\times 10^{-2}$) and (c) TCC of zirconolite compositions at room temperature and 1 MHz.

4. Conclusions

The complete subsolidus phase diagram of the system Bi_2O_3–ZnO–Ta_2O_5 has been determined at 950–1050 °C. The pyrochlore solid solutions form a trapezoidal-shaped compositional area, similar in size and location to that of the Nb_2O_5 system, but in this case, it includes the ideal nominal composition $Bi_{1.5}ZnTa_{1.5}O_7$; the area, confirmed by density measurements,[13] can be described by the general formula $Bi_{1.5+y/2}Zn_{1.0-x/2}Ta_{1.5-y/2}O_{7-x/2-y/2}$, The zirconolite phase forms a solid solution area that includes the ideal nominal composition, $Bi_2(Zn_{1/3}Ta_{2/3})_2O_7$. Systematic studies have been carried out to optimise sintering conditions (1100 °C) leading to high density pyrochlore ceramics; little composition-dependence of permittivity, dielectric loss and TCC is observed, although the dielectric loss appears to be least in samples with a stoichiometric Zn content, $x = 0$.

Acknowledgements

We thank EPSRC and Ministry of Science, Technology, and Innovation Malaysia (MOSTI) for financial support via IRPA Grant and NSF scholarship.

References

1. Boivin JC, Mairesse G. Recent material developments in fast oxide ion conductors. *Chem Mater* 1998;**10**:2870–88.
2. Kayed TS, Mergen A. Electrical properties of $Bi_{1.5}ZnSb_{1.5}O_7$ pyrochlore ceramics. *Crystallogr Res Technol* 2003;**38**:1077–81.
3. Subramanian MA, Aravamudan G, Subba Rao GV. Oxide pyrochlores: a review. *Prog Solid-State Chem* 1983;**15**:55–143.
4. Nino JC, Lanagan MT, Randall CA. Dielectric relaxation in Bi_2O_3–ZnO–Nb_2O_5 cubic pyrochlore. *J Appl Phys* 2001;**89**:4512–6.
5. Youn HJ, Randall C, Chen A, Shrout T, Lanagan MT. Dielectric relaxation and microwave dielectric properties of Bi_2O_3–ZnO–Ta_2O_5 ceramics. *J Mater Res* 2002;**17**:1502–6.
6. Randall CA, Nino JC, Baker A, Youn HJ, Hitomi A, Thayer R, et al. Bi-pyrochlore and zirconolite dielectrics for integrated passive component applications. *Am Ceram Soc Bull* 2003:9101–8.
7. Wang H, Yao X. Structure and dielectric properties of pyrochlore-fluorite biphase ceramics in the Bi_2O_3–ZnO–Nb_2O_5 system. *J Mater Res* 2001;**16**(1):83–7.
8. Youn HJ, Sogabe T, Randall CA, Shrout TR, Lanagan MT. Phase relations and dielectric properties in the Bi_2O_3–ZnO–Ta_2O_5 system. *J Am Ceram Soc* 2001;**84**:2557–61.
9. Levin I, Amos TG, Nino JC, Vanderah TA, Randall CA, Lanagan MT. Structural study of an unusual cubic pyrochlore $Bi_{1.5}Zn_{0.92}Nb_{1.5}O_{6.92}$. *J Solid State Chem* 2002;**168**:69–75.
10. Wang H, Du HL, Peng Z, Zhang ML, Yao X. Improvement of sintering and dielectric properties on Bi_2O_3–ZnO–Nb_2O_5 pyrochlore ceramics by V_2O_5 substitution. *Ceram Int* 2004;**30**:1225–9.

11. Tan KB, Lee CK, Zainal Z, Miles GC, West AR. Stoichiometry and doping mechanism of the cubic pyrochlore phase in the system Bi_2O_3–ZnO–Nb_2O_5. *J Mater Chem* 2005;**15**:3501–6.
12. Vanderah TA, Levin I, Lufaso MW. An unexpected crystal-chemical principle for the pyrochlore structure. *Eur J Inorg Chem* 2005:2895–901.
13. Khaw CC, Lee CK, Zainal Z, Miles GC, West AR. Pyrochlore phase formation in the system Bi_2O_3–ZnO–Ta_2O_5. *J Am Ceram Soc* 2007;**90**(9):2900–4.
14. Ling HC, Yan MF, Rhodes WW. High dielectric constant and small temperature coefficient bismuth-based dielectric compositions. *J Mater Res* 1990;**5**(8):1752–62.
15. Wang XL, Wang H, Yao X. Structure, phase transformation, and dielectric properties of pyrochlores containing bismuth. *J Am Ceram Soc* 1997;**80**:2745–8.
16. Levin I, Amos TG, Nino JC, Vanderah TA, Reaney IM, Randall CA, et al. Crystal structure of the compound $Bi_2Zn_{2/3}Nb_{4/3}O_7$. *J Mater Res* 2002;**17**:1406–11.
17. Tan KB, Lee CK, Zainal Z, Khaw CC, Tan YP, Shaari H. Reaction study and phase formation in Bi_2O_3–ZnO–Nb_2O_5 ternary system. *Pac J Sci Technol* 2008;**9**(2):468–79.
18. Tan KB, Khaw CC, Lee CK, Zainal Z, Miles GC. Structures and solid solution mechanisms of pyrochlore phases in the systems Bi_2O_3–ZnO–$(NbTa)_2O_5$. *J Alloys Compd* 2010;**508**:457–62.
19. Ling CD, Withers RL, Schmid S, Thompson JG. A review of bismuth-rich binary oxides in the systems Bi_2O_3–Nb_2O_5, Bi_2O_3–Ta_2O_5, Bi_2O_3–MoO_3, and Bi_2O_3–WO_3. *J Solid State Chem* 1998;**137**:42–61.
20. Safronov GM, Batog VM. Equilibrium diagram of the bismuth oxide–zinc oxide system. *Russ J Inorg Chem* 1971;**16**(3):460–1.
21. Rubia MA, Fernandez JF, Caballero AC. Equilibrium phases in the Bi_2O_3-rich region of the ZnO–Bi_2O_3 system. *J Eur Ceram Soc* 2005;**25**:2215–7.
22. Khaw CC, Tan KB, Lee CK. High temperature dielectric properties of cubic bismuth zinc tantalite. *Ceram Int* 2009;**35**:1473–80.
23. Nobre MAL, Lanfredi S. Dielectric spectroscopy on $Bi_3Zn_2Sb_3O_{14}$ ceramic: an approach based on the complex impedance. *J Phys Chem Solids* 2003;**64**:2457–64.
24. Mergen A, Lee WE. Crystal chemistry, thermal expansion and dielectric properties of $(Bi_{1.5}Zn_{0.5})(Sb_{1.5}Zn_{0.5})O_7$ pyrochlore. *Mater Res Bull* 1997;**32**:175–89.
25. Du HL, Yao X. Structural trends and dielectric properties of Bi-based pyrochlores. *J Mater Sci: Mater Electron* 2004;**15**:613–6.
26. Du HL, Yao X. Investigations on structural evolution and dielectric characteristics of high performance Bi-based dielectrics. *Mater Res Bull* 2005;**30**:1–9.
27. Wang H, Elsebrock R, Schneller T, Waser R, Yao X. Bismuth zinc niobate ($Bi_{1.5}ZnNb_{1.5}O_7$) ceramics derived from metallo-organic decomposition precursor solution. *Solid State Commun* 2004;**132**:481–6.